Progress In Electromagnetics Research C, Vol. 45, 137–150, 2013

DESIGN ULTRA-WIDE BANDWIDTH MONOPOLE ANTENNA FOR DVB-T AND WIRELESS APPLICATIONS

Dalia M. Elsheakh* **and Esmat A. Abdallah**

Electronics Research Institute, Microstrip Department, Giza, Egypt

Abstract—A novel shape of printed monopole antenna with a combination of Minkowski gasket and Koch fractal technique is presented in this paper. The ultra-wide bandwidth (UWB) antenna is composed of a modified ground plane with two independent elements as cross and Egyptian arc shapes to improve the antenna bandwidth. PIN diode is used to connect or disconnect the circular arc between two bands to switch frequencies from 500 to 2500 MHz and from 4 to 10 GHz. This implemented antenna effectively support personal communication system (PCS 1.85–1.99) GHz, universal mobile telecommunication system (UMTS 1.92–2.17) GHz, wireless local area network (WLAN), which usually operate in the 2.4 GHz (2.4–2.484 GHz) and 5.2/5.8 GHz (5.15–5.35 GHz/5.725–5.825 GHz) bands, mobile worldwide interoperability for microwave access and WiMAX, which operate in the range from 2.305 to 2.360 GHz, from 2.5 to 2.69 GHz and from 5.25 to 5.85 GHz bands. The properties of the antenna as reflection coefficient, efficiency, radiation patterns and gain are simulated and approved by the experimental results.

1. INTRODUCTION

With the rapid development of wireless technology of wireless communication networks, it is expected that the fourth generation technology is needed to meet this serves. This technology also offers the ability to access high-quality voice, and high data rate wireless and mobile devices [1–3]. Fourth mobile generation system focuses on faultless integration of existing wireless technologies including WWAN, WLAN and Bluetooth. The fourth generation intends to integrate from satellite broad band to high altitude platform cellular

Received 27 August 2013, Accepted 28 October 2013, Scheduled 8 November 2013

* Corresponding author: Dalia M. Elsheakh (daliaelsheakh@gmail.com).

2G and 3G system to wireless local loop (WLL) and broadband wireless access (BWA) to WLAN and wireless personal area networks (WPAN), all with IP as the integrating mechanism. This technology is used broadly to include several types of broadband wireless access communication systems, not only cellular systems [4]. Another type of this generation is Long-term evolution (LTE) is one of the 4th generation mobile communication technologies developed at different frequencies ranging from 500 MHz to 3 GHz. For UWB antenna, unlike single resonance printed antenna or monopole antennas, some special design considerations have to be taken into account. Instead of operating frequency, lower band-edge frequency and total bandwidth achieved become the design parameters. The lower band-edge frequency depends primarily on maximum height of the monopole according to equations in [5–7], whereas bandwidth of the antenna depends on how impedance of various modes is matched with the feed line. There are varieties of approaches that have been developed over the years, which can be utilized to achieve one or more of these design objectives. The developing of the antenna design objective has been improved by using fractal concept [8–10].

The advantages of the fractal antenna geometries are compact size and multiband frequency operations. The antenna design by using the fractal technique known as Minkowski gasket and the Koch curves printed monopole antenna is presented in [11–13]. This fractal antenna was created by iterating the initial square pulse through a monopole antenna. Next, a miniaturization of loop antenna using the semicircular arc as Egyptian arc, at the end of the monopole antenna is used to achieve lower band with modified ground plane [14, 15].

Ideal switch model is firstly used to imitate PIN diode switches with the opened (OFF) and closed (ON) states. This is approximately the same area of a real PIN diodes switch. Then the practical model of the PIN diode HPND-4005 is used for forward biased with 0.7 V and 10 mA [16]. It Exhibits an ohmic resistance of 3 Ω and intrinsic capacitance of 0.1 pF for forward bias, while exhibits 2.7 K ohm and 9 pF at 0 V. 10 pF capacitors are used as shown in Fig. 7(e), to isolate the RF signal from the DC and RF choke coil MCL 50–10000 MHz [17, 18]. Same PIN diode [19, 20] connections are used to connect and disconnect the arc to the main monopole antenna.

In this paper, the attributes of compact size and multiband in fractal properties is applied for a patch monopole antenna, which is created by modifying the technique of Kuch fractal concept designed for the reduction of antenna size with modified ground plane as shown in Fig. 1. PIN diode is used to connect or disconnect the lower band switch.

This paper is organized as follows: section one is an introduction of the paper work. While section two describes the antenna configuration and section three shows the antenna parametric studies and finally section four explains the experimental results and discussion.

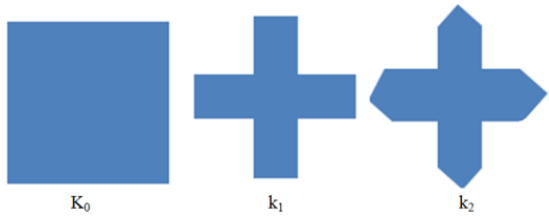

Figure 1. The steps of fractal shape; K_0: Initial shape, K_1: Minkowski gasket and k_2: Koch curves.

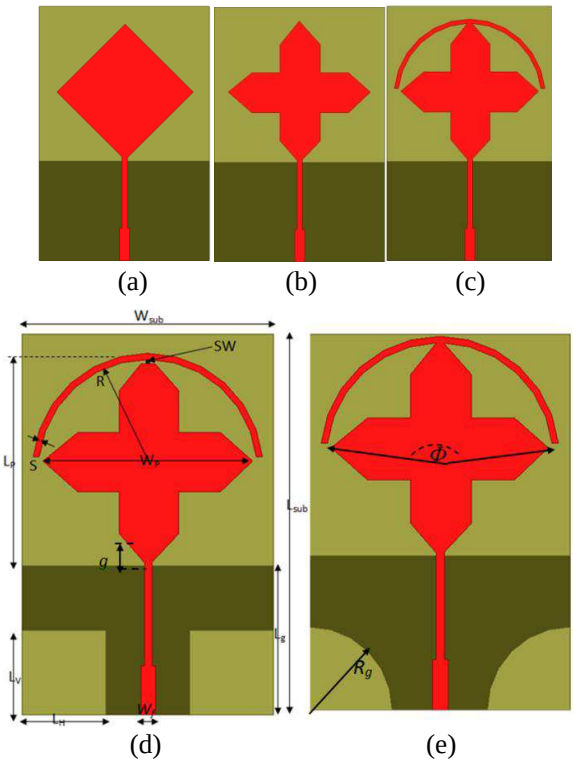

Figure 2. (a) to (e) The geometry and configuration of the proposed antenna design steps.

2. ANTENNA DESIGN CONFIGURATION

In this section, the proposed printed monopole antenna is created by etching Minkowski gasket shape and then etching Koch curve fractal monopole and modifying the ground plane which is optimized to improve the operating bandwidth. To reduce the lower frequency band or adding an extra band, an Egyptian arc is added to the monopole antenna. The configuration of the proposed antenna, as illustrated in Fig. 2, is a koch monopole antenna with a modified ground plane. The antenna consists of a radiating patch with a patch width W_p, which is fed by a microstrip line to match 50 Ω impedance with a strip width W_t on the top layer, and a modified ground plane of the antenna placed beneath the radiating patch on the bottom layer to improve the impedance bandwidth and radiation performances at high frequency.

The dimensions of the modified ground plane include the widths W_{sub}, R, R_g and the lengths L_g, L_V, L_H, L_p, strip Egyptian arc S. The design of the proposed monopole antenna steps is started by square patch shape monopole antenna with modified ground with L_g as step one in Fig. 3(a). First Minkowski gasket fractal is etched on squared shaped monopole antenna then Koch curve fractal is presented as step two in Fig. 3(a). Step three is adding Egyptian arc to improve the bandwidth as shown in Fig. 3(a). Step four is etching rectangular slot to create modified ground plane as shown in Fig. 3(a). Step five is changing the modified ground plane to circular shaped as shown in Fig. 3(a). The comparison between two modified ground plane shapes is shown in Fig. 3(b). Fig. 3(b) shows that the comparison of $|S_{11}|$ of

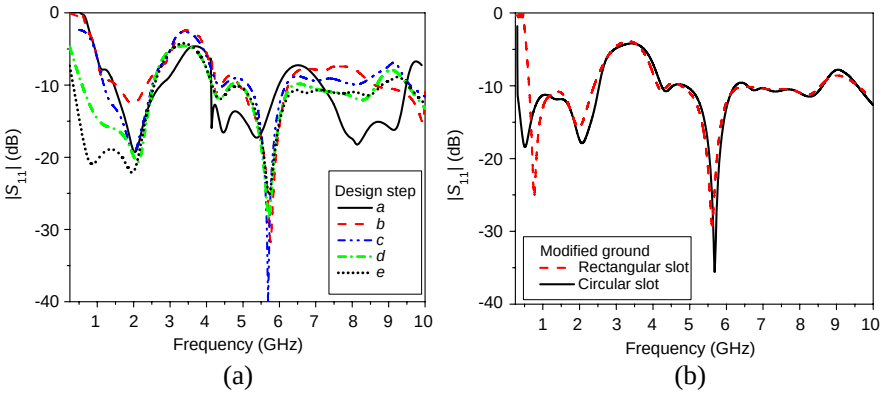

Figure 3. (a) The simulated $|S_{11}|$ of the design steps, (b) effect of ground plane shapes.

the circular ground plane gives wider bandwidth then square shapes and this is attributed to the fact that smoothing curvature improves antenna bandwidth. PIN diode is located between the monopole and Egyptian arc.

The proposed antenna is printed on an economical FR4 dielectric with a thickness of $h = 1.6\,\text{mm}$, relative permittivity of $\varepsilon_r = 4.4$, and loss tangent of 0.02. The total dimensions of the antenna are $60 \times 80 \times 1.6\,\text{mm}^3$. A $50\,\Omega$ SMA connector is used to feed the antenna at the microstrip line of radiating patch, in which the approximate width $W_t = 3.48\,\text{mm}$ and length $L_f = 36.5\,\text{mm}$ are fixed as shown in Fig. 2.

3. ANTENNA PARAMETRIC STUDY

Printed monopole antenna has dimensions of $60 \times 50\,\text{mm}^2$ and is placed on the top metallic layer of the antenna to cover the operating frequency bands of 1.2 GHz, 2.1 GHz, 2.3 GHz, 2.45 GHz, 2.5 GHz,

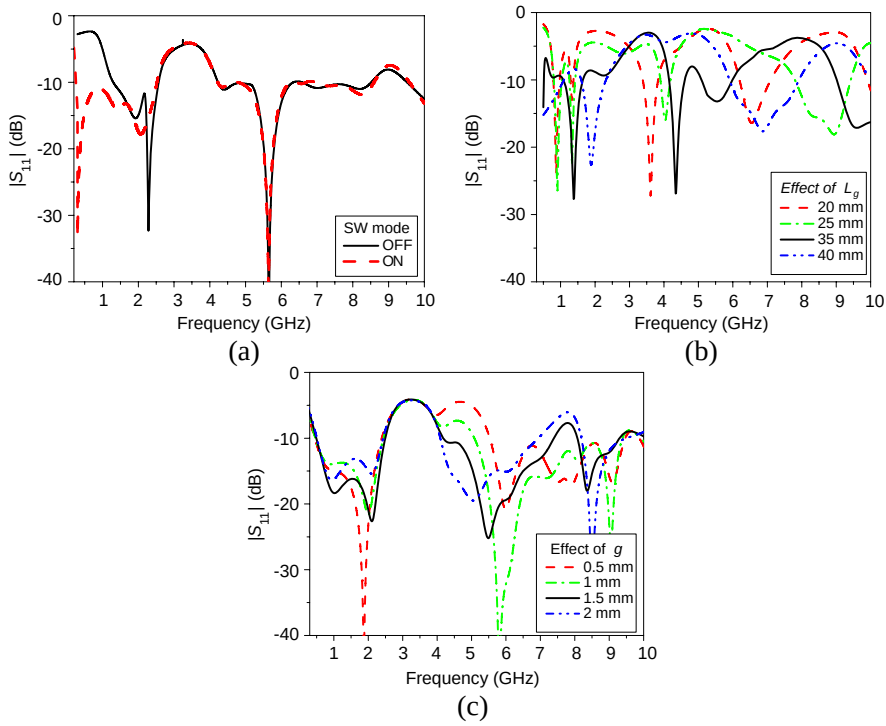

Figure 4. The effect of (a) SW modes (ON/OFF), (b) L_g, and (c) g on the antenna reflection coefficient.

bandwidth extended from 4 GHz to 10 GHz when SW is (OFF) and added extra band from 400 MHz to 1 GHz when SW is (ON). The comparison of reflection coefficient in the two switch modes (ON/OFF) is shown in Fig. 4(a). In order to improve the bandwidth of the higher band, the parameter L_g, was optimized from 20 mm to 40 mm with step 5 mm as shown in Fig. 4(b). The effect of separation between the monopole patch and the modified ground plane is shown in Fig. 4(c). The significant parameters, which influence the resonant frequencies as L_v, L_H, W_t, Φ are shown in Figs. 5 and 6. The slot length and width L_V, L_H are increased from 16 mm to 28 mm with step 4 mm and

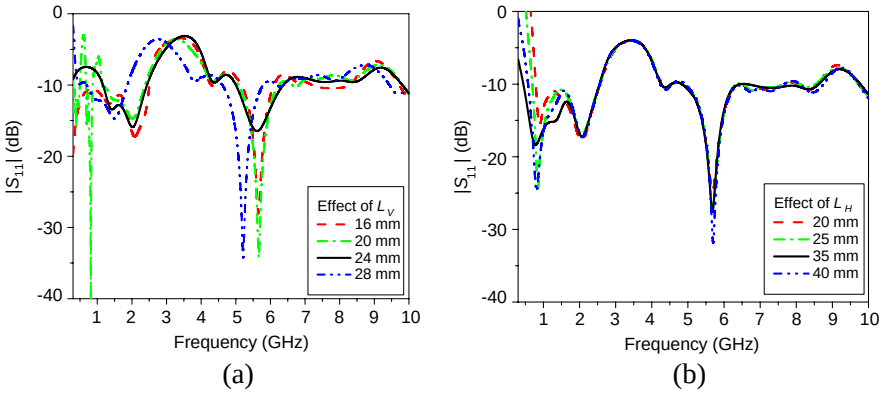

Figure 5. 5 Effect of (a) L_v and (b) L_H on the antenna bandwidth response.

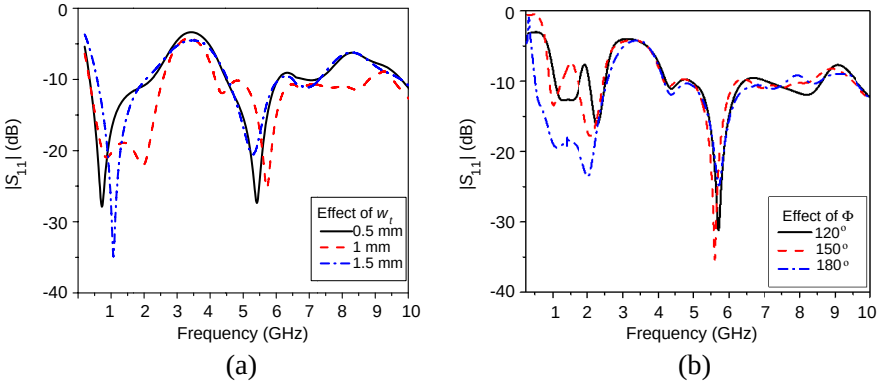

Figure 6. The effect of (a) W_t and (b) the angle Φ on antenna bandwidth.

from 20 mm to 40 mm with step 5 mm, respectively. The impedance matching at all resonant frequencies can be greatly improved.

Additionally, another effect of the modified ground plane on the radiation characteristic is W_t and it is investigated as shown in Fig. 6(a). W_t is another significant parameter for the impedance bandwidth matching at all resonant frequencies. The effect of the parameter W_t is investigated by varying W_t from 0.89 to 1.75 mm, as

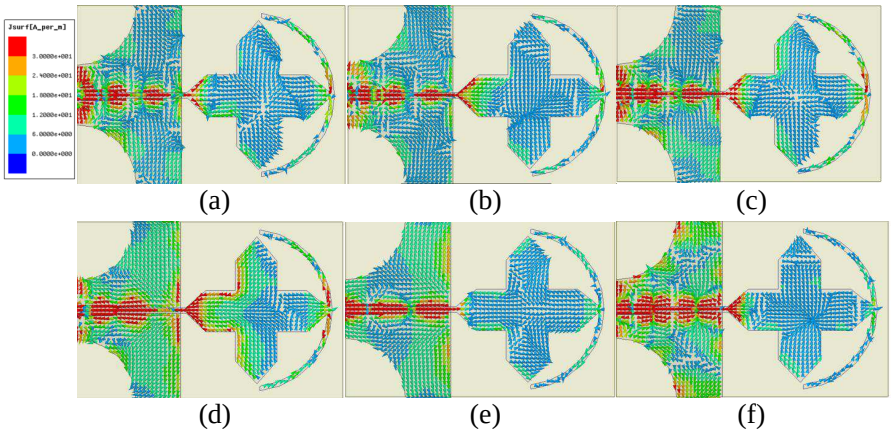

Figure 7. The surface current distribution at (a) (0.5), (b) 0.9 GHz, (c) 1.8 GHz, (d) 2.4 GHz, (e) 5.2 GHz, and (f) 10 GHz, respectively.

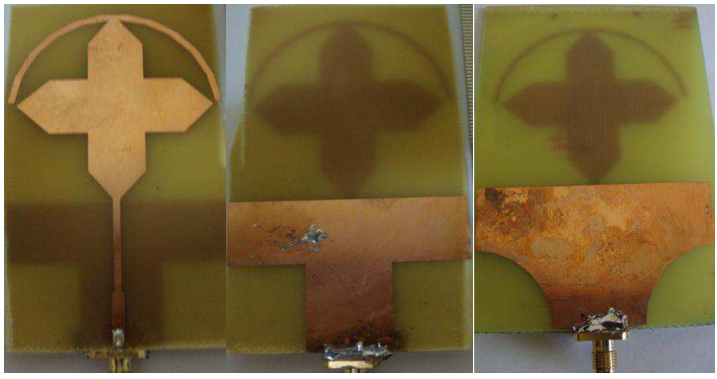

Figure 8. Photo of the fabricated antenna, (a) upper layer, (b) lower layer and circular ground.

shown in Fig. 6(a). As W_t increases, it can be clearly observed that the reflection coefficient. While the effect of the Egyptian arc angle Φ from 120° to 180° with step 30 degree are shown in Fig. 6(b).

The operations of the antenna at the wide band resonant frequencies are further studied using the surface current distribution as shown in Fig. 7. The antenna no longer acts as a fractal monopole mode at 2.4 GHz, and start resonant band from 3.5 GHz to 10 GHz. However the Egyptian arc at reasonable on the resonant at 500 MHz, 0.9 GHz and 1.8 GHz, as shown in Figs. 7(a) and (f). The highest current densities mainly flow around each element that corresponding to their resonant frequency, and so are responsible for the corresponding radiations.

Additionally, another effect of the modified ground plane on

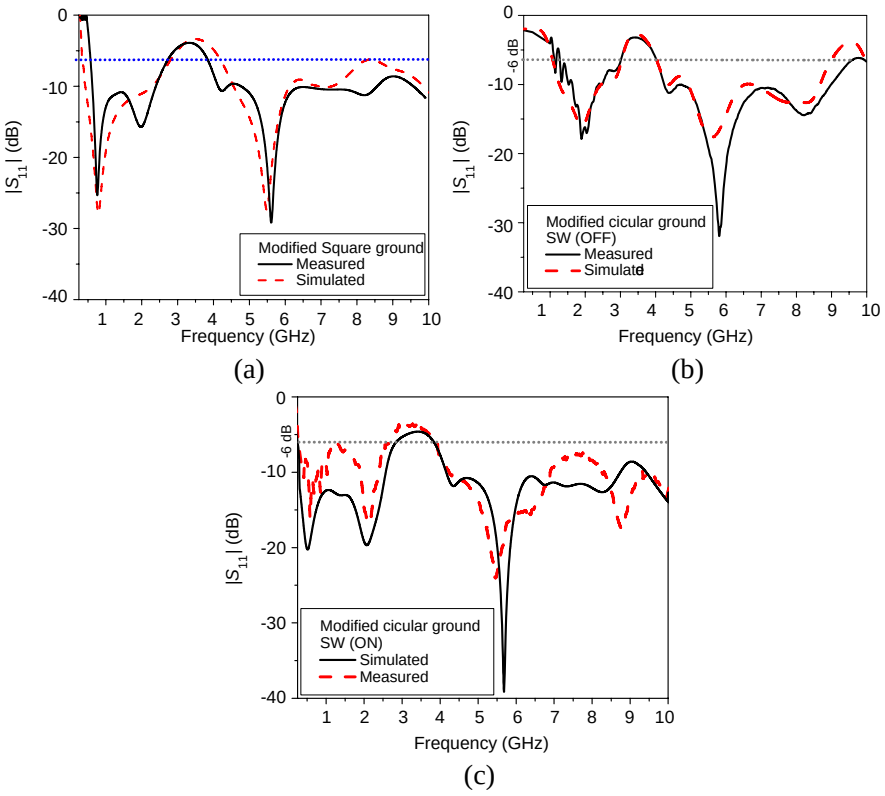

Figure 9. Comparison between measured and simulated $|S_{11}|$, (a) modified square ground shaped, (b) modified circular ground shape SW/ON, and (c) SW/OFF.

the radiation characteristic is investigated. Normally, in a low frequency band, the radiation pattern of the proposed antenna is effectively omnidirectional, but it has usually been deteriorated in a high frequency region, i.e., at the operating frequency of 10 GHz. The distorted pattern at high frequency is caused by the magnetic current mainly distributed over the gap between the radiating patch and the ground plane. The traveling waves move through the gap, resulting in directional radiation patterns in the horizontal plane (XZ-plane). By presenting the modified ground plane, the transverse currents on it are

Table 1. The simulated parameters of the proposed antenna at different resonant frequencies.

Resonance frequency (GHz)	0.5	0.9	1.8	2.4	5.2	10
Gain (dBi)	1.7	2	2.5	3.5	5.5	7.6
Sim. Radiation Efficiency (%)	75	80	85	85	85	90
Mea. Radiation Efficiency (%)	70	75	80	77	88	70

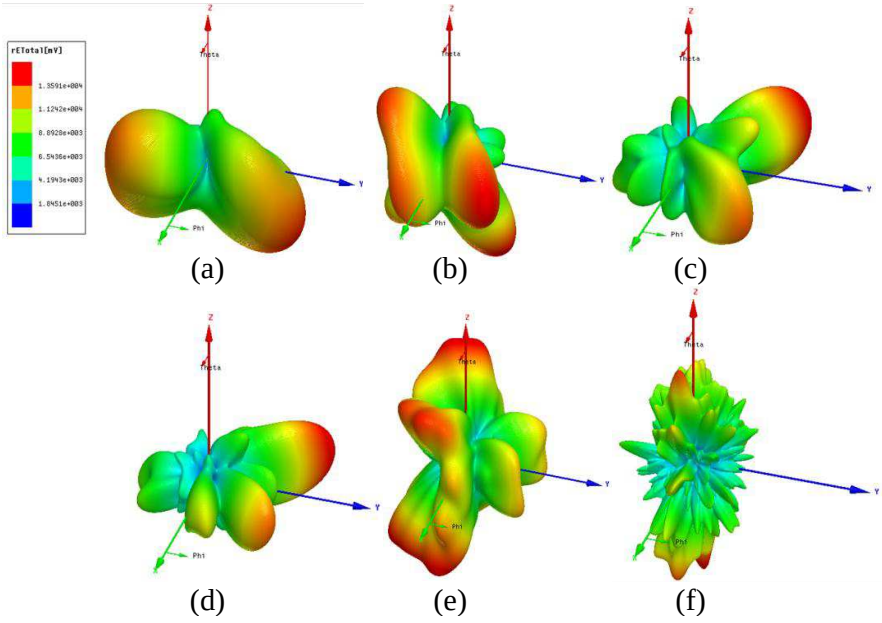

Figure 10. The simulated 3D radiation pattern at different resonant frequencies 0.5, 0.9, 1.8, 2.4, 5.2 and 10 GHz.

improved comparing with a rectangular ground plane. The current distribution at different frequencies is shown in Fig. 7. Therefore, at the high frequencies about 5 GHz, the currents on the modified ground plane are rearranged, then more power is fed into the gap between the radiating patch and the modified ground plane to radiate the waves from the gap, resulting in the propagation of an improved omnidirectional pattern. As a result, the gain at high frequency is around 7 dBi while in lower frequency is about 3.6 dBi as shown in Table 1.

4. EXPERIMENTAL RESULTS AND DISCUSSION

From the investigation of various parameters that affect the operating frequency bands of the proposed antenna in the previous section, the appropriate parameters including $W = W_g = 59\,\text{mm}$, $L = 90\,\text{mm}$, $L_g = 35.25\,\text{mm}$, $W_s = 33.54\,\text{mm}$, $L_t = 25.36\,\text{mm}$, $W_t = 3.48\,\text{mm}$, $L_f = 11.55\,\text{mm}$, $L_{p1} = 16.14\,\text{mm}$, $L_{p2} = 36.02\,\text{mm}$, $L_{p3} = 6.21\,\text{mm}$, $L_{p4} = 7.45\,\text{mm}$, $g = 1.15\,\text{mm}$, $L_{gt} = 17.6\,\text{mm}$, $L_{gf} = 17.65\,\text{mm}$, $W_{gt} =$

Table 2. The measured radiation pattern in ZX and XY planes at the resonant frequencies E_Φ: black solid lines, E_Θ: black dotted lines.

F (GHz)	XZ	XY
0.5	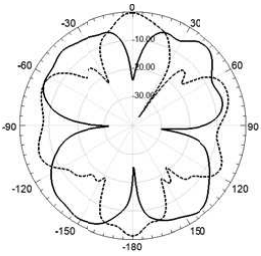	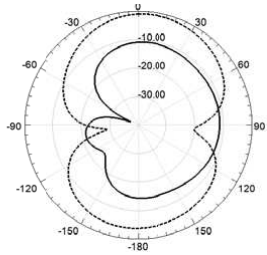
0.9	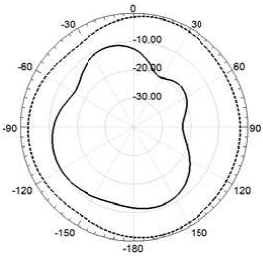	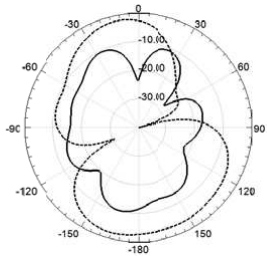

1.8	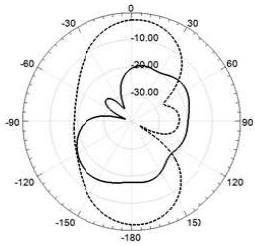	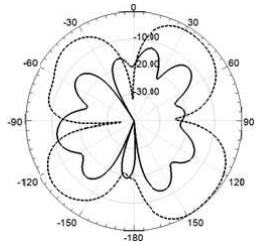
2.4	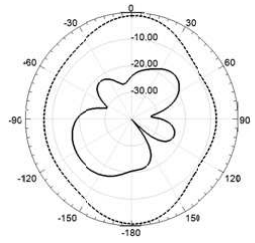	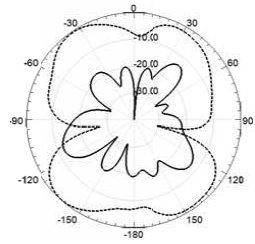
5.2	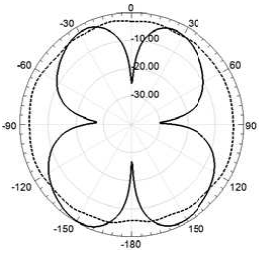	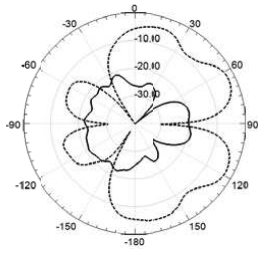
10	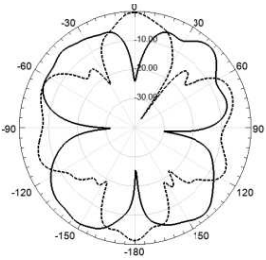	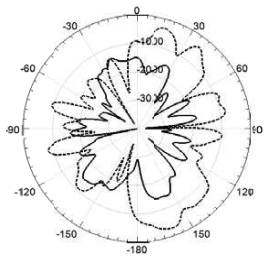

21 mm, $W_{gf} = 17$ mm, and width of strip feed, $W_f = 1.41$ mm are selected to construct the prototype antenna by etching into chemicals, as shown in Fig. 8. Fig. 9 shows simulated and measured return losses of the optimal proposed antenna. The simulated result shows three resonant frequencies at 2.13 GHz, 4.46 GHz, and 5.56 GHz, while the measured result has similarly resonant frequencies at 2.17 GHz, 4.47 GHz, and 5.6 GHz.

The 3D radiation patterns of the original design simulated at some in-band frequencies are plotted as shown in Fig. 10. These chosen frequencies are located at 0.5 GHz, 0.9 GHz, 1.8 GHz, 2.4 GHz, 5.2 GHz and 10 GHz in the operating band of this antenna. The radiation patterns of the proposed antenna are measured with Star-Lab 18 anechoic chamber. The measured 2D polar radiation patterns at the same resonant frequencies are shown in Table 2. As this figure and table indicate that the radiation patterns keep good directivity with slight change through the whole frequency band and all the back lobes are below −15 dB. However, the side lobes deteriorate with the increase of frequency, especially in the high frequency bands, such as 10 GHz. The measured and simulated radiation efficiency at selected frequencies in the operating band is summarized in Table 1. The radiation efficiency was measured by using wheeler-cap method [21, 22].

5. CONCLUSION

In this paper, combination of Minkowski gasket and Koch fractal printed monopole antenna was investigated. The PIN diode switch is used to connect and disconnect on Egyptian arc to add or eliminate the lower band. The geometrical parameters of the proposed antenna have been optimized to enhance the impedance bandwidth to operate in most of wireless communication system bands. The proposed antenna has an omnidirectional radiation patterns at all of the operating frequency bands which makes it suitable for using in wireless communication applications.

ACKNOWLEDGMENT

This research is supported by the National Telecommunication Regularity Authority (NTRA), Ministry of Communication and Information Technology, Egypt.

REFERENCES

1. Song, Y., Y.-C. Jiao, G. Zhao, and F.-S. Zhang, "Multiband CPW-fed triangle-shaped monopole antenna for wireless applications," *Progress In Electromagnetics Research*, Vol. 70, 329–336, 2007.
2. Elsadek, H. and D. M. Nashaat, "Compact size trapezoidal PIFA antenna," *Journal of Electromagnetic Waves and Applications*, Vol. 21, No. 7, 865–876, 2007.

3. Liu, W. C. and H.-J. Liu, "Miniaturized asymmetrical CPW-fed meandered strip antenna for triple-band operation," *Journal of Electromagnetic Waves and Applications*, Vol. 21, No. 8, 1089–1097, 2007.
4. Ang, B.-K. and B.-K. Chung, "A wideband E-shaped microstrip patch antenna for 5–6 GHz wireless communications," *Progress In Electromagnetics Research*, Vol. 75, 397–407, 2007.
5. Wang, F. J. and J.-S. Zhang, "Wide band cavity-backed patch antenna for PCS/IMT2000/2.4 GHz WLAN," *Progress In Electromagnetics Research*, Vol. 74, 39–46, 2007.
6. Eldek, A. A., A. Z. Elsherbeni, and C. E. Smith, "Characteristics of bow-tie slot antenna with tapered tuning stubs for wideband operation," *Progress In Electromagnetics Research*, Vol. 49, 53–69, 2004.
7. Eldek, A. A., A. Z. Elsherbeni, and C. E. Smith, "Design of wideband triangle slot antennas with tuning stub," *Progress In Electromagnetics Research*, Vol. 48, 233–248, 2004.
8. Pazin, L., N. Telzhensky, and Y. Leviatan, "Wideband flat-plate inverted-F laptop antenna for WI-FI/WIMAX operation," *IET Microw Antennas Propag.*, Vol. 2, No. 6, 568–573, Sep. 2008.
9. Tang, I.-T., D.-B. Lin, W.-L. Chen, and J.-H. Horng, "Miniaturized hexaband meandered PIFA antenna using three meandered-shaped slits," *Microwave and Optical Technology Letters,* Vol. 50, No. 4, 1022–1025, Apr. 2008.
10. Li, F., L.-S. Ren, G. Zhao, and Y.-C. Jiao, "Compact triple band monopole antenna with C-shaped and S-shaped meander strips for WLAN/WiMAX applications," *Progress In Electromagnetics Research Letters*, Vol. 15, 107–116, 2010.
11. Ren, X., X. Chen, and K. M. Huang, "A novel electrically small meandered line antenna with a trident-shaped feeding strip for wireless applications," *International Journal of Antennas and Propagation*, Vol. 2012, 1–7, 2012.
12. Qu, S. W., C. L. Ruan, and Q. Xue, "A planar folded ultrawideband antenna with gap-loading," *IEEE Trans. Antennas Propag.*, Vol. 55, No. 1, 216–220, Jan. 2007.
13. Ray, K. P. and Y. Ranga, "Ultrawideband printed elliptical monopole antennas," *IEEE Trans. Antennas Propag.*, Vol. 55, No. 4, 1189–1192, Apr. 2007.
14. Dastranj, A., A. Imani, and M. Naser-Moghaddasi, "Printed wide-slot antenna for wideband applications," *IEEE Trans. Antennas Propag.*, Vol. 56, No. 10, 3097–3012, Oct. 2008.

15. Liu, W. C. and F. M. Yeh, "Compact dual-and wide-band CPW-fed slot antenna for wireless applications," *Microwave and Optical Technology Letters*, Vol. 50, No. 3, 574–575, Mar. 2008.
16. Avago Technologies, "HPND-4005 beam lead PIN diode," Oct. 2006.
17. Feng, T., Y. Li, H. Jiang, W. Li, F. Yang, X. Dong, and H. Chen, "Tunable single negative metmaterial based on microstrip transmission line with varactor diode loading," *Progress In Electromagnetics Research*, Vol. 120, 35–50, 2011.
18. Mak, A. C. K., C. R. Rowell, R. D. Murch, and C.-L. Mak, "Reconfigurable multiband antenna designs for wireless communication devices," *IEEE Trans. Antennas Propag.*, Vol. 55, No. 7, 1919–1928, Jul. 2007.
19. Anagnostou, D. and A. Gheethan, "A coplanar reconfigurable folded slot antenna without bias network for WLAN applications," *IEEE Antennas Wireless Propag. Lett.*, Vol. 8, 1057–1060, 2009.
20. AbuTarboush, H. F., R. Nilavalan, S. W. Cheung, K. M. Nasr, T. Peter, D. Budimir, and H. Al-Raweshidy, "A reconfigurable wideband and multiband antenna using dual-patch elements for compact wireless devices," *IEEE Trans. Antennas Propag.*, Vol. 60, No. 1, 36–43, Jan. 2012.
21. Hohnston, R. H. and J. G. McRory, "An improved small antenna radiation efficiency measurement method," *IEEE Antennas and Propagation Magazine*, Vol. 40, No. 5, 40–48, Oct. 1998.
22. Raiva, A. P. and J. F. Sanchez, "A rectangular cavity for cell phone antenna efficiency measurement," *IEEE Antennas and Propagation Society International Symposium*, Vol. 2B, 740–743, 2005.